RSC Advances

ROYAL SOCIETY OF CHEMISTRY

www.rsc.org/advances

RSC Advances

RSCPublishing

ARTICLE

Disk-Like Nanojets with Steerable Trajectory Using Platinum Nozzle Nanoengines †

Cite this: DOI: 10.1039/x0xx00000x

Liangxing Hu,[a] Jianmin Miao*[a] and Gerhard Grüber*[b]

Self-propelled disk-like nanojets are proposed and illustrated, consisting of non-catalytic gold (Au), central magnetic nickel (Ni) and catalytic nozzle platinum (Pt). This innovative type of the Au-Ni-Pt nanojets with either one off-center or two identically and symmetrically distributed Pt nozzle nanoengines are for the first time designed and fabricated using an easy-operation layer-by-layer deposition method based on nano-electro-mechanical systems (NEMS) technology, whereby Pt functions as the chemical catalyst for the decomposition of hydrogen peroxide (H_2O_2) to produce oxygen (O_2) bubbles detaching from the surface and water (H_2O), which in turn generates a recoil force thrusting the nanojets propelling forward. The propulsion mechanism originated from the momentum change of a Au-Ni-Pt nanojet-oxygen bubble integral system and the steerable trajectories of the two different shaped nanojets are investigated. Moreover, the nanojet's motion is characterized and recorded in diluted H_2O_2 solution under an optical microscope, revealing that the O_2 bubbles are generated and detached from the surface of Pt catalyzing H_2O_2 decomposition. In addition, the novel Au-Ni-Pt nanojets with one off-center Pt nanoengine can autonomously propel forward circularly, while the Au-Ni-Pt nanojets with two identically and symmetrically distributed Pt nozzle nanoengines can move forward in a linear way.

Received 00th,
Accepted 00th

DOI: 10.1039/x0xx00000x

www.rsc.org/advances

Introduction

Nanomotor is a nanoscale device, which has the capability to convert energy into mechanical movement or force.[1] In nature, living systems possess their intelligent and efficient bio-molecular motor proteins for various functions through millions of years of evolution.[2] Microorganisms are able to drive themselves through aqueous media with the aid of mechanical conformational deformation of their own solid appendages using the energy they harvest from the surrounding environments.[3] For instance, bacteria are capable of propelling forward using the rotational flagellar nanomotors, which are powerful molecular nanomotors, transforming ion motive force (IMF) into rotary kinematic motion.[4] Moreover, linear bio-molecular nanomotors, such as kinesin, myosin and dynein, can couple hydrolysis of adenosine triphosphate (ATP) into adenosine diphosphate (ADP) and phosphate (Pi) for lateral movement along the corresponding tracts (actin or microtubule filaments), in order to transport numerous functional cargoes *in vivo*.[5,6] In addition, biological cells are equipped with molecular engines, which are required to generate the biological fuel ATP. These engines are the rotary molecular nanomotors of F- and A-ATP synthases. Both of them consist of two distinct reversible rotary motors that can operate in different types of fuel. One is a soluble motor (F_1 or A_1 motor), which synthesizes ATP molecules. The other one is a hydrophobic transmembrane motor (F_o or A_o motor), which is powered by the concentration gradient of biochemical ions (H^+, Na^+) as well as functions like a turbine.[7-8]

Evolution bestows bio-molecular motor proteins with the fascinating ability to harvest energy from surrounding environments for the autonomous functions *in vivo* described above. Inspired by naturally occurring molecular nanomotors, researchers extensively devoted great efforts into artificial nanodevices in last few decades. They tried to design and fabricate devices, which could possess the ability to mimic the functions of bio-molecular nanomotors existing in living bodies. For example, Gibbs and his co-workers reported a Pt-coated silica sphere, called Janus nanomotor, catalyzing H_2O_2 to propel the motion in diluted H_2O_2 solution in 2009.[9] Another similar work was carried out by Ebbens and his colleagues in which a nonconductive Janus particle swimmer was proposed, which constituted a fluorescent polymer bead coated with a hemisphere of Pt.[10] Samuel and his co-workers developed the smallest man-made jet engine via the rolled-up nanotech method.[11]

The aforementioned artificial catalytic devices coated with Pt can autonomously propel forward in aqueous solution in the

presence of H_2O_2.[9-11] To date, there are several mechanisms to explain the aforementioned motion phenomena, such as self-electrophoresis, interfacial tension and self-diffusiophoresis.[12-15] These mechanisms mainly focused on the chemical reaction process of the decomposition of H_2O_2 to explain the locomotion of the nanodevices. Less attention has been paid to the nano-device's motion induced by the momentum change. In this paper, self-propelled nanojets with two different shapes are proposed, which consist of tri-metallic components: non-catalytic Au, central magnetic Ni and catalytic Pt nozzle nanoengine. A bubble propulsion mechanism originated from the momentum change, generated by the detachment of the O_2 bubbles from the Pt-surface, is proposed to explain the locomotion of the Au-Ni-Pt nanojets. On the other hand, the rolled-up technique and electrochemical method have been exploited to fabricate the hollow cylindrical and conical nanojets with such high complexity, and these two methods need much higher skills for operation.[11, 16-18] Meanwhile, a long-term aim is to develop and fabricate the nanojets in a low-cost and high-efficiency manner, as well as suitable of applying in bio-sensing, environmental remediation and drug delivery.[19-21] Herein, the proposed disk-like nanojets are fabricated using an easy-operation and high-efficiency layer-by-layer deposition method based on NEMS technology. Moreover, the steerable trajectories of the fabricated nanojets are experimentally characterized and recorded under a microscope, revealing that the O_2 bubbles are generated and detached from the surface of the Pt nozzle nanoengines. In addition, the nanojets with one off-center Pt nanoengine can autonomously propel forward in a circular way, while the Au-Ni-Pt nanojets with two identically and symmetrically distributed Pt nozzle nanoengines can move forward translationally.

Bubble propulsion mechanism and steerable trajectory of the nanojets

The autonomous propulsion of the disk-like Au-Ni-Pt nanojets in aqueous H_2O_2 solution is induced through the detachment of the O_2 bubbles from the Pt-surface, as illustrated in Fig. 1. The H_2O_2 decomposition in general can be described as

$$2H_2O_2 \xrightarrow{Pt} 2H_2O+O_2 \quad (1)$$

where, Pt represents the catalyst platinum.[9-11, 13] Herein, H_2O_2 is firstly adsorbed onto the surface of Pt, then decomposes into H_2O and O_2 bubbles.[22]

Before adding H_2O_2, the nanojets are relatively stationary in deionized (DI) water. Once H_2O_2 added into DI water, the O_2 bubbles are generated (growing state) and then detached (detaching state) from the surface of Pt, as shown in Fig. 1(a). According to the Momentum Conservation Law and Momentum Theorem, a recoil force F_{drive} (ESI†), as shown in Fig. 1(b) and (c), will be generated to initiate and accelerate the nanojet's motion due to the detachment of the O_2 bubbles. On the other hand, the man-made rockets can orbit around earth and realize the steerable trajectories using self-equipped jet engines in the space. Hence, the proposed nanojets with one off-center Pt nozzle nanoengine, as shown in Fig. 1(b), will propel forward circularly, because the recoil force F_{drive} and the viscous drag force F_{drag} are not in a line, due to the generated O_2 bubbles are not symmetrically distributed along the horizontal axes of the nanojets. While the nanojets with two identically and symmetrically distributed Pt nozzle nanoengines, as shown in Fig. 1(c), will move forward translationally, because F_{drive} and F_{drag} are totally balanced resulting from the generated O_2 bubbles are symmetrically and identically distributed. At the steady state, F_{drive} is equal to F_{drag}, thus the Au-Ni-Pt nanojets reach a constant velocity of v.

Experimental section

Fabrication of disk-like Au-Ni-Pt nanojets with Pt nozzle nanoengines

The schematic composition, size and structure of the nanojets before being released from 4 inch thick silicon (Si) wafer are shown in Fig. 2. Au and Ni are shaped as a disk with 12 μm in diameter. The thicknesses of Au- and Ni-disks are 200 nm and 100 nm, respectively. The Pt nozzle nanoengine forms a hollow cylinder. The diameter, thickness and height of the Pt nozzle are 2 μm, 300 nm and 1.5 μm, respectively. Pt is used as the catalyst to chemically decompose H_2O_2 into both H_2O and O_2 bubbles.[22] Au is used as the non-catalyst and purposely to build asymmetric structure for ensuring autonomous propulsion in th-

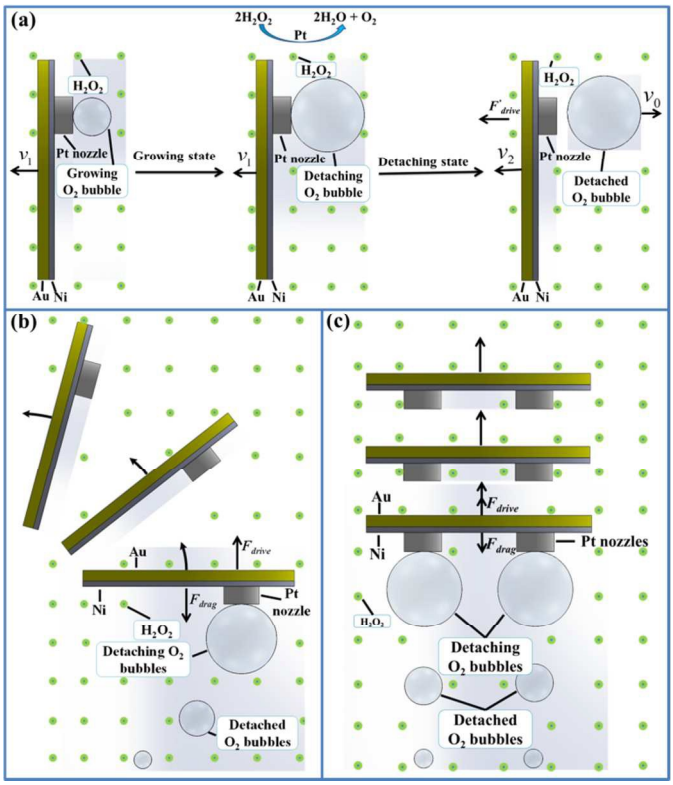

Fig. 1 Schematic diagram depicting the motion mechanism and the steerable trajectories of the disk-like Au-Ni-Pt nanojets immersed into H_2O_2 solution. (a) Illustration of the Au-Ni-Pt nanojet's propulsion originating from the momentum change, due to the detachments of the O_2 bubbles from H_2O_2 decomposition catalyzed by Pt; (b) and (c) representation of the circular motion of the Au-Ni-Pt

nanojets with one off-center Pt nozzle nanoengine and linear motion of the Au-Ni-Pt nanojets with two identically and symmetrically distributed Pt nozzle nanoengines in H_2O_2 solution, respectively.

e micro and nanoscale regime. Ni is magnetic material for controlling the propulsion in further work. For instance, the motion direction of a Ni-contained nano-object can be controlled under an external magnetic field.[23-24] The fabrication process has been carried out using mature developed NEMS technology in the Micromachines Lab, School of Mechanical and Aerospace Engineering (MAE) at Nanyang Technological University (NTU), Singapore. The detailed fabrication steps are illustrated in Fig. 3.

To fabricate the structure, a 4 inch Si wafer was firstly immersed into sulfuric acid (H_2SO_4) to clean the surface at 120°C for 30 minutes. The Si wafer surface was then deposited with a layer of 1 μm thick silicon dioxide (SiO_2) by plasma enhanced chemical vapor deposition (PECVD) at 300°C for 40 minutes. In order to improve photoresist adhesion on oxides, SiO_2 coated Si wafer was transferred into a prime oven for hexamethyldisilazane (HMDS) coating to form a strong chemical bond onto the surface of SiO_2 in 2 minutes. Subseque-

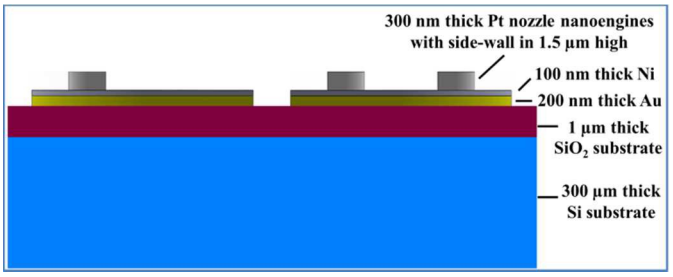

Fig. 2 Schematic diagram demonstrating the structure, composition and size of the Au-Ni-Pt nanojets with two different shapes on Si wafer. The proposed nanojets are composed of three components: 200 nm thick Au (golden yellow color), 100 nm thick Ni (black color) and 300 nm thick Pt nozzle nanoengines (gray color) with side-wall in 1.5 μm high, the left hand-side one is the nanojet with one off-center Pt nozzle nanoengine and the right hand-side one is the nanojet with two identically and symmetrically distributed Pt nozzle nanoengines, respectively.

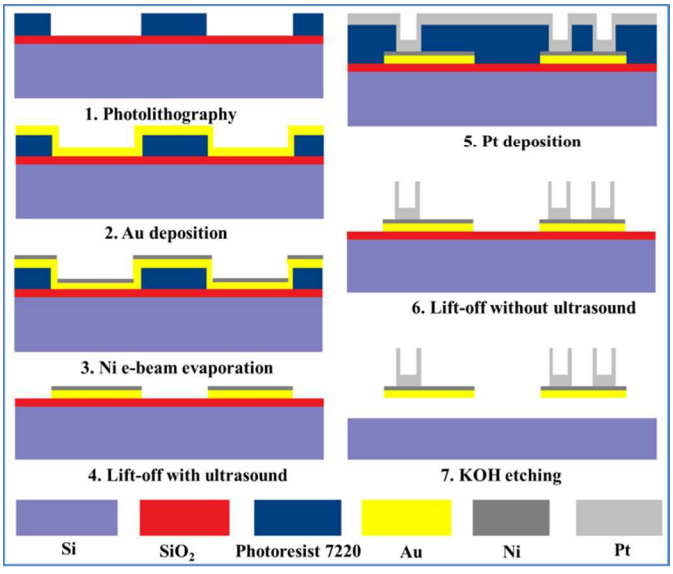

Fig. 3 Diagram of the fabrication process of the disk-like Au-Ni-Pt nanojets. The nanojets are fabricated using the easy-operation layer-by-layer deposition method based on NEMS technology, including PECVD, photolithography, sputtering, e-beam evaporation, lift-off and KOH etching.

ntly, a layer of 1.5 μm thick photoresist 7220 was spin-coated on the SiO_2 surface at 5000 revolutions per minute (rpm) over 30 seconds. Thereafter, the pattern on the glass photomask was exposed onto the photoresist 7220 coated Si wafer under 365 nm wavelength ultraviolet (UV) light in 4 seconds. The pattern was developed in an AZ 300MIF developer solution for 1 minute. The patterned Si wafer was firstly coated with a layer of 200 nm thick Au by magnetron sputter in 9 minutes, following coated with a layer of 100 nm thick Ni with e-beam evaporation for 15 minutes. Afterwards, the wafer was immersed into acetone etching off photoresist, called *lift-off*. The photolithography process was done once again, a 300 nm thick Pt-layer was subsequently coated onto the surface by magnetron sputter for 9 minutes. Lastly, the Au-Ni-Pt nanojet arrays were formed on the SiO_2 surface by lift-off without ultrasound. The nanojets were released by etching off 1 μm thick SiO_2 using potassium hydroxide (KOH). The fabricated Au-Ni-Pt nanojets were stored in a glass bottle for the following experiments.

The scanning electron microscopy (SEM) images of the fabricated Au-Ni-Pt nanojets with either one off-center or two identically and symmetrically distributed Pt nozzle nanoengines on Si wafer surface are shown in Fig. 4(a) and (b), respectively. The corresponding energy dispersive spectrometry (EDS) analysis results of the disk plate and the nozzle nanoengines of the two different shaped nanojets are revealed in Fig. 5. From the EDS analysis, one can obtain the distribution and the percentage of Au, Ni and Pt elements.

O_2 bubble generation

The experimental set-up was established to study the nanojet's motion (ESI†). The fabricated Au-Ni-Pt nanojets immersed into aqueous H_2O_2 solution were dropped on the surface of glass slide using a pipette. The prepared sample was transferred onto the microscope stage. Afterwards, the motion of the Au-Ni-Pt nanojets was captured by the microscope equipped with the camera. Finally, the motion process was recorded by the computer installed with a video recording software. It could be observed that the O_2 bubbles were continuously generated at the Pt-surface with the addition of H_2O_2 into DI water, as shown in Fig. 6. The O_2 bubbles were detached from the Pt-surface after a period of time. The recoil force, induced by the detachment of the O_2 bubbles, thrust the nanojets propelling autonomously forward towards the Au part. The diameters of the O_2 bubbles at the nanojets' surfaces were approximated to be 60 μm, as shown in Fig. 6(a) and (b), when the bubbles were detaching. The results were in good agreement with those described by Wang and Wu.[25]

Au-Ni-Pt nanojet's steerable motion in H_2O_2 solution

The fabricated Au-Ni-Pt nanojets, as shown in Fig. 4, were immersed into diluted H_2O_2 solution to observe the steerable motion. The time lapses for the circular and linear motion

processes of the two distinct shaped nanojets were characterized and recorded, as shown in Fig. 7(a) and (b), respectively. The software "ImageJ" was utilized to process the recorded data of the nanojet's motion, and the corresponding circular and linear steerable trajectories of the nanojets were obtained, as shown in Fig. 8(a) and (b), respectively.

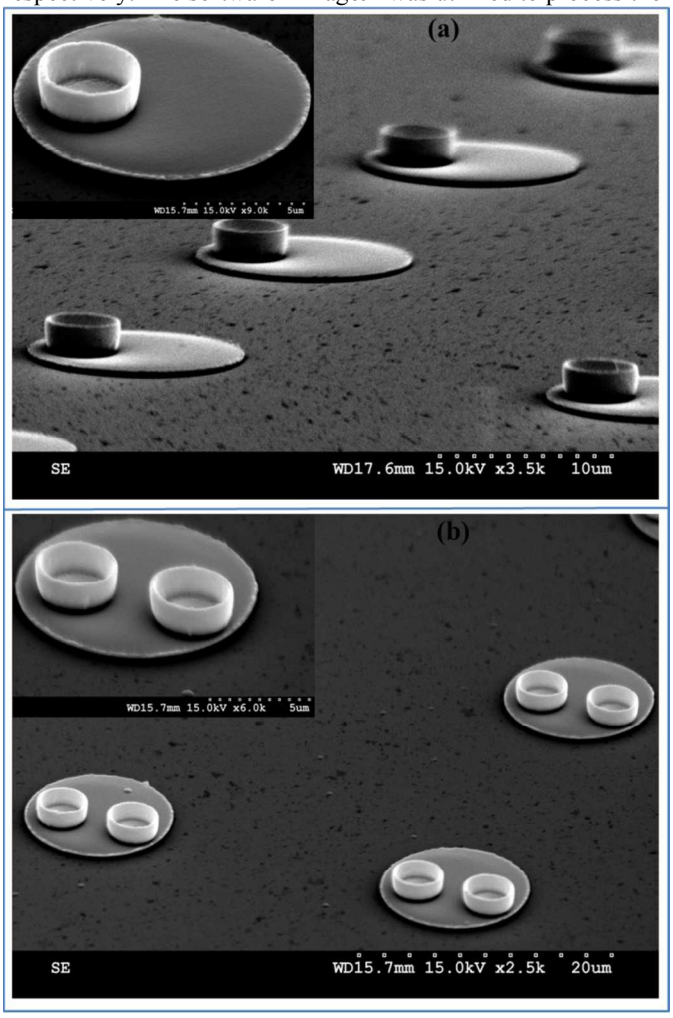

Fig. 4 SEM images of the fabricated Au-Ni-Pt nanojets. SEM side views of the fabricated Au-Ni-Pt nanojets with either one off-center (a) or two identically and symmetrically distributed (b) Pt nozzle nanoengines. The inlets show the enlarged Au-Ni-Pt nanojets in two different shapes.

Results and discussion

It has been investigated that the nanodevices could move forward towards[12-14] or backward from the non-catalyst[9-11]. The proposed Au-Ni-Pt nanojets presented above reveal a forward movement, consistent with the results described in reference 9-11, 25. Moreover, the data obtained in this study demonstrated that H_2O_2 was chemically catalysed by Pt and decomposed into both O_2 bubbles and H_2O. The generated O_2 bubbles detached from the Pt-surface (Fig. 6-7) proved that Pt can be acted as the catalyst for the decomposition of H_2O_2.

Au-Ni-Pt nanojet's motion speed in H_2O_2 solution

In the experiments described above, the moved time t, as presented in Fig. 7, and moved distance L, as shown in Fig. 8, were obtained from the recorded videos. The unit of the distance and speed are μm and μm/s, respectively. Thus, the motion speeds v of the Au-Ni-Pt nanojets can be calculated as.[26]

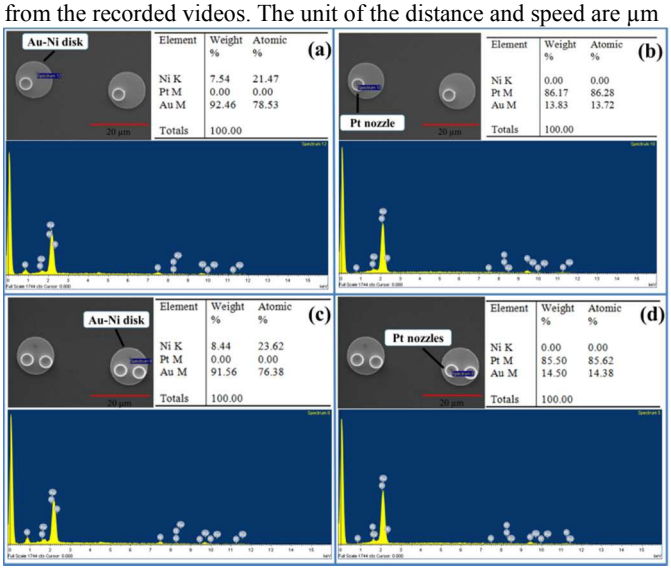

Fig. 5 EDS analysis results of the two different shaped Au-Ni-Pt nanojets. (a) and (b) show EDS analysis results on the disk plate and the nozzle nanoengine of the Au-Ni-Pt nanojet with one Pt nozzle nanoengine, respectively; (c) and (d) present EDS analysis results on the disk plate and the nozzle nanoengines of the Au-Ni-Pt nanojet with two Pt nozzle nanoengines, respectively.

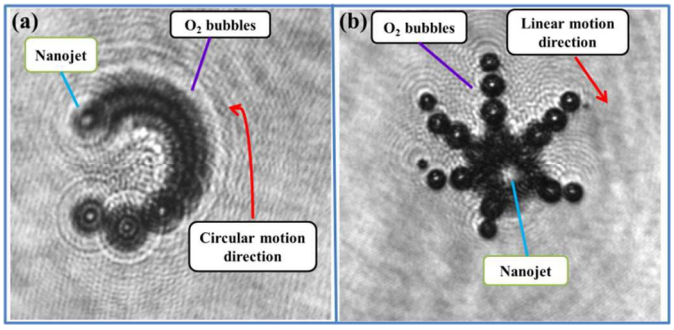

Fig. 6 Steerable motion of the Au-Ni-Pt nanojets. (a) Circular motion of the Au-Ni-Pt nanojet with one Pt nozzle nanoengine and (b) linear motion of the Au-Ni-Pt nanojet with two Pt nozzle nanoengines in H_2O_2 solution, respectively.

$$v = \frac{L}{t} \quad (2)$$

The Au-Ni-Pt nanojet's steerable motion was studied in diluted H_2O_2. The calculated speed of the nanojets with one off-center Pt nozzle nanoengine was about 200 μm/s, as shown in Fig. 7(a) and 8(a). While the motion speed for the nanojets with two identically and symmetrically distributed Pt nozzle nanoengines was approximated to be 80 μm/s, as demonstrated in Fig. 7(b) and 8(b). Due to the differences from the nanojets' shape and material composition, the aforementioned speeds were larger than those presented in reference 11. In fact, the nanojets would undergo thermal fluctuation motion, called Brownian motion. The speed of the Brownian motion (ESI†) was much smaller than the motion speeds presented above.

Au-Ni-Pt nanojet's steerable trajectory in H_2O_2 solution

The fabricated two different shaped Au-Ni-Pt nanojets with Pt Pt nozzle nanoengines, as shown in Fig. 4, were dispersed into diluted H_2O_2 solution to observe the steerable trajectories. It was observed that the nanojets with one off-center Pt nozzle nanoengine autonomously propelled forward circularly in diluted H_2O_2 solution, while the nanojets with two identically and symmetrically distributed Pt nozzle nanoengines moved forward in a translational way. The time lapses for the two different shaped nanojets' circular and linear motion were shown in Fig. 7(a) and (b), respectively. Moreover, the recorded data was processed using the software "ImageJ" to obtain the corresponding steerable trajectories of the two different shaped nanojets, as shown in Fig. 8(a) and (b), respectively.

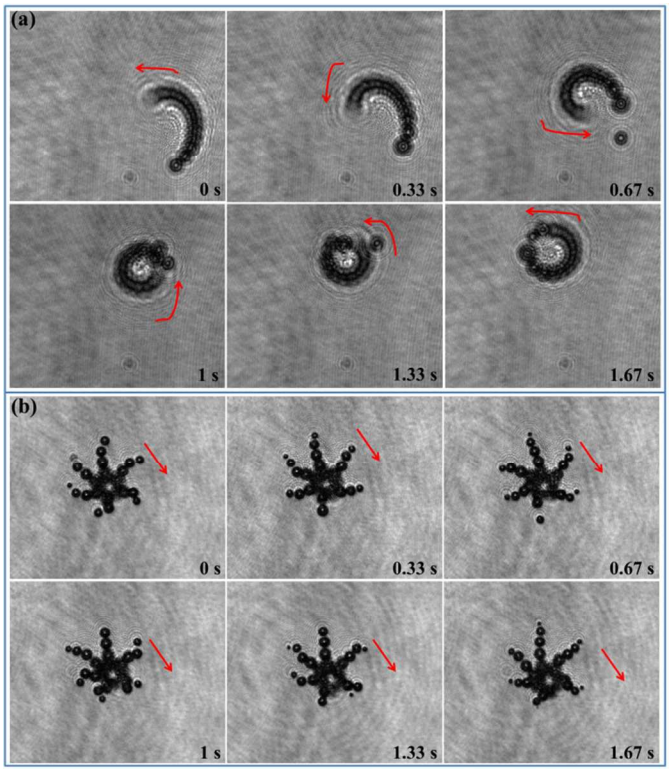

Fig. 7 Time lapses of the Au-Ni-Pt nanojets. (a) Time lapses of the circular motion of the Au-Ni-Pt nanojet with one Pt nozzle nanoengine and (b) time lapses of the linear motion of the Au-Ni-Pt nanojet with two Pt nozzle nanoengines in H_2O_2 solution, respectively.

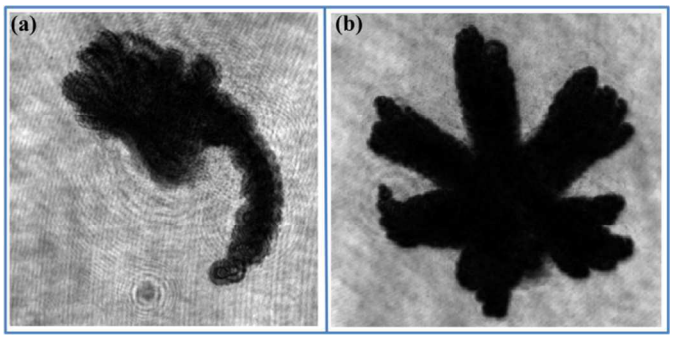

Fig. 8 Trajectories of the Au-Ni-Pt nanojets. (a) Trajectory of the Au-Ni-Pt nanojet with one Pt nozzle nanoengine and (b) trajectory of the Au-Ni-Pt nanojet with two Pt nozzle nanoengines in H_2O_2 solution, respectively.

Discussion on disk-like Au-Ni-Pt nanojet's motion

The pressure difference Δp at the interface between two fluids can be described by the Young-Laplace equation,[25] thus the pressure inside the O_2 bubbles P_{O_2} can be calculated as follows

$$P_{O_2}=P_{atm}+\Delta p \quad (3)$$

where, P_{atm} =1.015×10^5 Pa is the atmospheric pressure.

In our experiments, it was obtained that about 50 O_2 bubbles were generated and detached from the surface of the Pt nanoengine over 1 minute (Fig. 6 and 7), and the speed of the detached O_2 bubbles from the Au-Ni-Pt nanojets was about 80 μm/s.[25] Based on the values given above, the pressure inside the O_2 bubbles can be calculated using equation (3). Using the equation derived by Gibbs and his colleague,[9] one can obtain that the catalytic reaction rate constant k is about 128.1 mol/(m^2·s) and the adsorption constant α is approximately 0.067 m^3/mol for the nanojets. The results were in good agreement with those shown in reference 9. On the other hand, the motion speeds in our results were much lower than those presented by other researchers,[23, 24] resulting from the different materials and shapes of the nanojets. In such a case, one can learn the reasons in reference 9. In fact, there are several parameters influencing the final speeds of the nanojets, giving us the guidance how to design, optimize and investigate the nanomtors in future work.

In the aforementioned results, it was observed that the fabricated nanojets with one off-center Pt nanoengine moved forward in a circular way, while the nanojets with two identically and symmetrically distributed Pt nozzle nanoengines propelled forward translationally. Herein, the mechanism of the nanojet's steerable trajectory was proposed and studied. At steady state, if the generated O_2 bubbles and geometry of the nanojets were definitely symmetrical along the horizontal axes of the nanojets, *i.e.* F_{drive}=F_{drag}, F_{drive} and F_{drag} were in a line along the horizontal axes of the nanojets, no torque was generated and the nanojets would undergo the linear motion, as shown in Fig. 9(a). On the other hand, if the generated O_2 bubbles were not equally and symmetrically distributed along the horizontal axes of the nanojets, even though F_{drive} = F_{drag}, they were not in a line, then a torque Q was generated, which would further lead to the nanojets propelling forward circularly with a motion radius R_c, as shown in Fig. 9(b). In conclusion, at steady state, if F_{drive} and F_{drag} were in a line, no torque was generated and the nanojets moved forward linearly. Otherwise, the torque Q was generated and the nanojets would propel forward circularly.

Conclusions

The bubble propulsion mechanism stemmed from the momentum change induced by the detachment of the O_2 bubbles from the surface of the catalyst Pt was proposed to investigate the propulsion of the Au-Ni-Pt nanojets with Pt

nozzle nanoengines in H_2O_2 solution. Moreover, the efficient and mass-production layer-by-layer deposition method was for the first time utilized to fabricate the two different shaped Au-Ni-Pt nanojets with Pt nozzle nanoengines based on NEMS technology. The steerable motion of the disk-like Au-Ni-Pt nanojets was experimentally investigated in diluted H_2O_2 solution. In addition, the results demonstrated that the nanojets with one off-center Pt nozzle nanoengine could move forward circularly in H_2O_2 solution due to the presence of a torque, while the nanojets with two identically and symmetrically distributed Pt nozzle nanoengines could propel forward translationally. The results of this research will encourage further studies, such as the exploration of the steerable trajectories of the nanojets via the geometry design of Pt nanoengines,[27] the motion observation of the nanojets placed in micro-channels[28] and the controlling by the external magnetic field[23, 24, 29, 30]. Such nanojets may be a promising for environmental sensing[19-20] and other applications[21, 31-33].

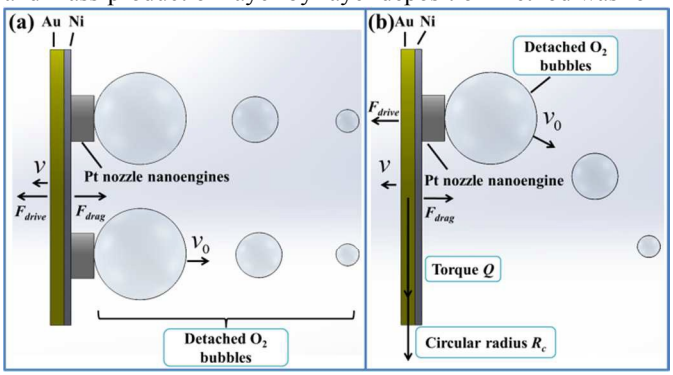

Fig. 9 Schematic diagrams for explaining the steerable motion of the disk-like Au-Ni-Pt nanojets. (a) Au-Ni-Pt nanojets with two identically and symmetrically distributed Pt nozzle nanoengines could move forward towards the Au-segments translationally. The forces F_{drive} and F_{drag} were in a line and the O_2 bubbles generated at the Pt-surface were also along the horizontal axes of the nanojets, which didn't induce a torque Q. (b) Diagram of the explanation of the circular motion of the Au-Ni-Pt nanojets with one off-center Pt nozzle nanoengine. The Au-Ni-Pt nanojets would propel forward in a circular way with a radius R_c, because the forces were not in a line, which would introduce an extra torque Q.

Acknowledgements

This work was financially supported by the Ministry of Education Tier 2 (Grant No: MOE2011-T2-2-156; ARC 18/12), Singapore. We also gratefully acknowledged Dr. Wu Jin to give his efforts on paper revision, Mr. Kai Tao to help draw the pictures, Mr. Pek and Mr. Nordin in Micromachines Lab, NTU, for their help on the nanomotor fabrication and SEM characterization.

Notes and references

[a]School of Mechanical and Aerospace Engineering, Nanyang Technological University, 50 Nanyang Avenue, Singapore, 639798. Email: mjmmiao@ntu.edu.sg
[b]School of Biological Sciences, Nanyang Technological University, 60 Nanyang Drive, Singapore, 639798. Email: ggrueber@ntu.edu.sg

† Electronic Supplementary Information (ESI) available: The videos of circular and linear motion of the nanojets; Equipment, materials and software used; the driving force derivation; experimental set-up; Brownian motion speed of the Au-Ni-Pt nanojets. See DOI: 10.1039/b000000x/

1 J. Wang, *ACS Nano*, 2009, **3**, 4-9.
2 C. Brennen and H. Winet, *Annu. Rev. Fluid Mech.*, 1977, **9**, 339-398.
3 G. T. Yates, *Am. J. Sci.*, 1986, **74**, 358-365.
4 D. Stock, K. Namba and L. K. Lee, *Curr. Opin. Biotechnol.*, 2012, **23**, 545-554.
5 C. Schmidt and V. Vogel, *Lab Chip*, 2010, **10**, 2195-2198.
6 S. K. Vashist, R. Tewari, I. Kaur, R. P. Bajpai and L. M. Baharadwaj, *Proceedings of ICISIP*, 2005, DOI: 10.1109/ICISIP.2005.1529495.
7 A. G. Stewart, M. Sobti, R. P. Harvey and D. Stock, *Bioarchitecture,* 2013, **3**, 2-12.
8 G. Grüber, M. S. Manimekalai, F. Mayer and V. Müller, *Biochem. Biophys. Acta-Bioenergetics,* 2014, **1837**, 940-952.
9 J. G. Gibbs and Y. P. Zhao, *Appl. Phys. Lett.*, 2009, **94**, 1-3.
10 S. J. Ebbens and J. R. Howse, *Langmuir*, 2011, **27**, 12293-12296.
11 S. Sanchez, A. Solovev, S. Harazim, C. Deneke, Y. Mei and O. Schmidt, *Chem. Rec.*, 2011, **11**, 367-370.
12 Y. Wang, R. M. Hernandez, D. J. Bartlett, J. M. Bingham, T. R. Kline, A. Sen and T. E. Mallouk, *Langmuir*, 2006, **22**, 10451-10456.
13 W. F. Paxton, K. C. Kistler, C. C. Olmeda, A. Sen, S. K. St. Angelo, Y. Cao, T. E. Mallouk, P. E. Lammert, V. H. Crespi, *J. Am. Chem. Soc.*, 2004, **126**, 13424-13431.
14 R. Golestanian, T. B. Liverpool and A. Ajdari, *Phys. Rev. Lett.*, 2005, **94**, 1-4.
15 B. Sabassa and U. Seifert, *J. Chem. Phys.,* 2012, **136**, 064508.
16 W. Gao, S. Sattayasamitsathit, J. Orozco and J. Wang, *J. Am. Chem. Soc.*, 2011, **133**, 11862-11864.
17 G. Zhao, A. Ambrosi and M. Pumera, *Nanoscale*, 2013, **5**, 1319-1324.
18 A. Martín, B. Jurado-Sánchez, A. Escarpa and J. Wang, *Small*, 2015, **11**, 3568-3574.
19 T. Li, L. Li, W. Song, L. Wang, G. Shao and G. Zhang, *ECS J. Solid State Sci. Technol.*, 2015, **4**, S3016-S3019.
20 M. Guix, J. Orozco, M. Garcı´, W. Gao, S. Sattayasamitsathit, A. Merkoci, A. Escarpa and J. Wang, *ACS Nano*, 2012, **6**, 4445-4451.
21 X. Yan, Q. Zhou, J. Yu, T. Xu, Y. Deng, T. Tang, Q. Feng, L. Bian, Y. Zhang, A. Ferreira and L. Zhang, *Adv. Funct. Mater.*, 2015, **25**, 5333-5342.
22 S. B. Hall, E. A. Khudaish and A. L. Hart, *Electrochim. Acta*, 1998, **43**, 579-588.
23 J. Li, Q. Xiao, J. Z. Jiang, G. N. Chena and J. J. Sun, *RSC adv.*, 2014, **4**, 27522-27525.
24 M. Safdar, T. Itkonen and J. Janis, *RSC adv.*, 2015, **5**, 13171-13174.
25 S. Wang and N. Wu, *Langmuir*, 2014, **30**, 3477-3486.
26 J. Bao, Z. Yang, M. Nakajima, Y. Shen, M. Takeuchi, Q. Huang, and T. Fukuda, *IEEE Trans. Robot.*, 2014, **30**, 33-39.
27 J. Li, G. Huang, M. Ye, M. Li, R. Liu and Y. Mei, *Nanoscale*, 2011, **3**, 5083-5089.
28 L. Soler, C. Martínez-Cisneros, A. Swiersy, S. Sánchez and O. Schmidt, *Lab Chip*, 2013, **13**, 4299–4303.
29 T. R. Kline, W. F. Paxton, T. E. Mallouk and A. Sen, *Angew. Chem. Int., Ed.*, 2005, **44**, 744-746.
30 G. A. Ozin, *ChemCatChem*, 2013, **5**, 2798-2801.

31 D. Kagan, R. Laocharoensuk, M. Zimmerman, C. Clawson, S. Balasubramanian, D. Kang, D. Bishop, S. Sattayasamitsathit, L. Zhang and J. Wang, *Small*, 2010, **6**, 2741-2747.
32 D. A. Wilson, R. J. M. Nolte and J. C. M. Hest, *Nat. Chem.*, 2012, **4**, 268-274.
33 W. Gao, R. F. Dong, S. Thamphiwatana, J. X. Li, W. W. Gao, L. F. Zhang and J. Wang, *ACS Nano*, 2015, **9**, 117-123.

A Graphical and Textual Abstract for the Table of Contents Entry

Liangxing Hu, Jianmin Miao and Gerhard Grüber

Nanojets with one off-center platinum nozzle nanoengine can propel forward circularly, while the nanojets with two identically and symmetrically distributed platinum nozzle nanoengines are capable of moving forward in a linear way.